TRANSONIC SMALL DISTURBANCE CODE FOR BODY - WING CONFIGURATION COUPLED WITH FULL POTENTIAL CODE FOR WING ALONE

A. Luntz
Israel Aircraft Industries, Ben Gurion Airport,
ISRAEL

ABSTRACT

A transonic small disturbance approximation code TSD was designed, for potential flow around a body-wing configuration. This code is based on the embedded fine grid concept elaborated by Ch. Boppe. Improvements are introduced into the boundary condition representation, including the body boundary condition, the wing boundary condition and the interface between the fine grid box and the coarse grid computation. Only cartesian coordinate grids are used. The code provides good prediction of the position of the shock on the wing surface, using a comparatively small number (about 20) of grid points along the wing section cord. The TSD code is coupled with a modified Jameson FL022 code. The symmetry condition (no crossflow at the wing root plane) in FL022, is replaced with the crossflow values computed by the TSD code. This new boundary condition, at the wing root, contains all information of the body influence needed for the wing pressure computation. The coupling allows detailed analysis of the body-wing interference effects in the flow.

1. The TSD Code

The small disturbance code (TSD) is based on the transonic small disturbance approximation.

Following [5], we solve the transonic small disturbance equation

$$\left[1-M_\infty^2-(\gamma+1)\cdot M_\infty^2\cdot\left(\varphi_x+\tfrac{1}{2}\varphi_x^2\right)\right]\varphi_{xx}-2M_\infty^2\varphi_y\varphi_{xy}+$$
$$+\left[1-(\gamma-1)M_\infty^2\varphi_x\right]\varphi_{yy}+\varphi_{zz}=0 \quad (1)$$

outside a computational cylinder which includes the body.

Here, φ is the perturbation potential $\varphi(x,y,z)$,

$$u=1+\varphi_x\ ,\quad v=\varphi_y\ ,\quad w=\varphi_z\ .$$

The TSD code uses the embedded fine grid concept and the slender body approximation introduced in [4], [5]. Unlike [5], this code uses only cartesian coordinate mesh grids. This is possible with improved small disturbance boundary conditions at the flat plate, representing the wing surface. The TSD code, like [4], [5], uses a coarse mesh grid representing the semispace, and a fine mesh grid covering an embedded box, for detailed analysis of the flow (Figs. 1, 2). Unlike [5], the TSD code uses, at each grid, alternative direction iterations and an improved way of exchanging information between the two grids. At each mesh grid, the TSD code uses, in the iteration process, the core memory only.

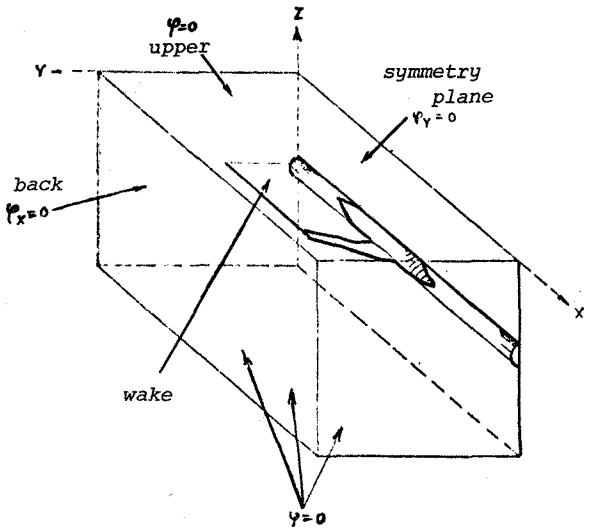

Fig. 1

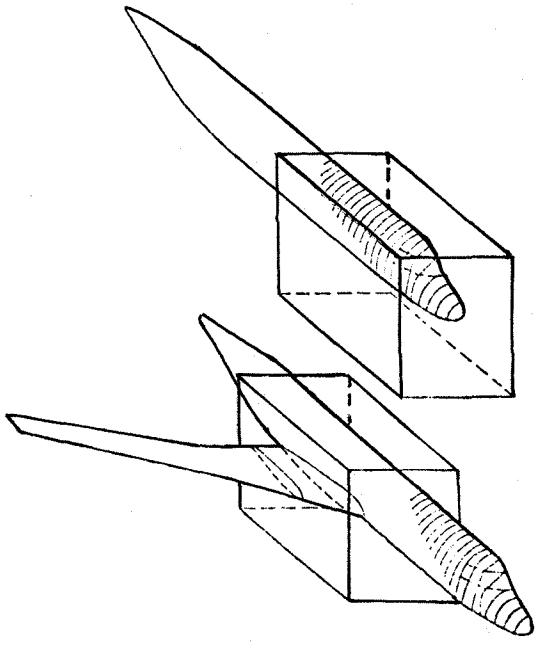

Fig. 2

The exchange of information between the two grids takesplace in the form of boundary conditions at the 5 faces of the fine grid box (the 6th lies on the symmetry plane). At each side, an input control parameter defines what information - potential, its derivative across the box face, or their combination - is calculated in one grid and provided to the other grid as boundary condition. In the opposite direction complementary information is provided as boundary condition at this box face. In most cases normal derivative is provided as boundary condition for the fine grid computation at all box faces except the front (upwind) face, where the potential value is given. In such cases the boundary condition computed in the fine grid and provided for the coarse grid iterations, is potential values at each fine grid box face, except for the front face, where the boundary condition for the coarse grid iteration is the potential derivative (flow across the face).

In the fine mesh grid, the mesh size usually used in the y, z directions is 2 to 3 times the mesh size in the x-direction. This bigger y and z mesh size proves to be enough for purposes of accuracy and helps to save memory and computational time. Stability in computation is guaranteed, first of all, by choosing proper directions of column solution and - if necessary - by relaxation parameters.

Typical fine mesh grids are 50x20x40 for body alone, 80x32x32 for body-wing configurations.

The computation usually takes about 30-50 full iteration cycles, each including 2-5 iteration sweeps on the coarse grid and 4-10 sweeps on the fine grid.

2. Boundary Conditions

Many efforts were made during the last decade ([1], [2], [3], [4] an others) to improve the solution of the small disturbance equation, by changing the equation itself, mostly by introducing additional terms. The boundary condition on the flat plate, representing the wing, remained

$$\varphi_z = f_x - \alpha \qquad (2)$$

where $z = f(x,y)$ is the wing surface (upper or lower), α - angle of attack.

In the present work it is proven that the inaccuracy of the small disturbance equation solution (compared with the full potential equation) is due mostly to the traditional wing boundary condition (2), not to the equation itself.

The following improvements are introduced in the TSD code:
(a) a more exact boundary condition is used:

$$\varphi_z/(1+\varphi_x) = f_x - \alpha \qquad (3)$$

to express the fact that streamlines of the flow should lie on the wing surface;
(b) the boundary condition (a) is imposed (implicitly) on the wing surface, not on the flat plate;
(c) at the leading edge, the mapping of the wing surface onto the flat plate is singular, so that the equation may be not applied in its original form. Special treatment is used at the leading edge, based on the incompressible flow approximation at this point.

Fig. 3 shows the Cp distribution over a supercritical wing section computed by different methods:
(*) using equation (1) and boundary condition (3),
(**) using equation (1) and boundary condition (2),
(***) using the simplified equation

$$[1-M_\infty^2-(\gamma+1)M_\infty^2\varphi_x]\varphi_{xx} + [1-M_\infty^2(\gamma-1)\varphi_x]\varphi_{yy}+\varphi_{zz}=0 \qquad (4)$$

and boundary condition (3).

Fig.3 shows that neglect of several terms in equation (1) spoils the solution less than the use of the innaccurate approximation (2) to the wing boundary condition.

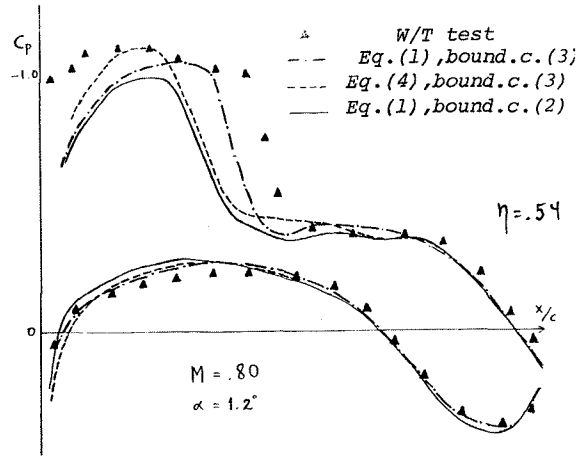

Fig. 3

In [5], the body boundary condition at the cylinder surface (which is the boundary of the computational space) is transferred from the body surface:

$$\left.\frac{\partial\varphi}{\partial n}\right|_{cyl.} = N_x\cdot\lambda + N_z\cdot\alpha\cdot\lambda^2, \qquad (5)$$

$$\lambda = R_B/R_C,$$

R_b (R_c) - body (cylinder) section radius, N_x, N_z - corresponding components of the normal to the body surface, - angle of attack. Boundary conditions (5) provide surprisingly good results (considering the roughness of the approximation (5)) for smooth body surfaces with not very high slopes ($|N_x| \leq 1/2$). For surface regions with high slopes (blunt nose) or angles - results computed with (5) are inaccurate.

One of the reasons for it is that equation (5) transports the singularities of the body surface into the interior of the flow field. To avoid that, the TSD code uses values of N_x and N_z (which appear in the right hand side and, implicity, in the left hand side of the equality (5)) averaged over a region, which is shifted from the original point in the x-direction. The size of the region and the shifting distance are proportional to $-N_x.(R_c-R_b)$.

3. Coupling with FLO22

For many configurations, the TSD code alone gives satisfactory results. Still, there are cases in which the TSD code is unsufficient, mostly for the following two reasons:

- although measures were taken to improve the TSD computation in the leading edge region, singular mapping of the wing surface onto the flat plate and not enough detailed meshing, around the leading edge, in cartesian coordinates, do not allow satisfactory representation of fast changes in the pressure coefficient at the leading edge;

- as mentioned above, the fine grid potential values remain, during one iteration, in the computer core memory. For wings with high aspect ratio, and with the computer used to run the TSD code, it becomes possible to cover only a part of the wing with a sufficiently fine grid.

This led us to couple the TSD code with the FLO22 code.

To make the coupling possible modifications had to be made in the FLO22 code. Instead of zero values of the potential derivative across the wing root plane (symmetry condition), imput values of this derivative are used in the modified code.

The whole computation proceeds as follows:
1) A body-wing configuration is calculated by the TSD code, the fine box grid covering all (or most of) the wing.
2) A plane parallel to the symmetry plane of the configuration is chosen, cutting the wing near the root, and the crossflow (the potential derivative normal to the plane) is computed.
3) This crossflow is interpolated to the FLO22 grid points, at the root, and then used as input to the modified FLO22.
4) FLO22 computation proceeds using the given crossflow at the wing root.

In principle, the computation cycle may be repeated by using the TSD code again, this time with the information from the FLO22 code of the potential values on a certain plane cutting the wing. But experiment shows that this second cycle does not lead to additional changes in the Cp distribution and thus is not necessary.

Using the TSD-FLO22 combination, not only detailed computation of the pressure distribution over body-wing comfigurations is possible, but also analysis of the sources of certain effects. Fig. 4 shows comparison of two runs of FLO22 for a supercritical swept wing of high aspect ratio in a low position. The effects produced by the body influence, namely the spanwise wind, can be seen. Among them are the rear shock at the inboard part of the wing and additional lift at all sections along the span.

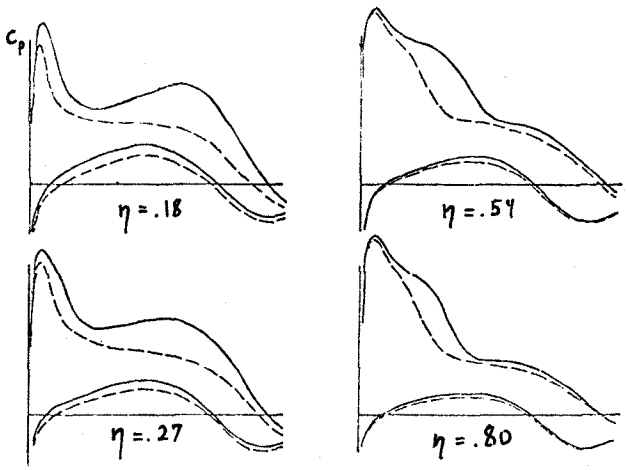

M = .80 ---- FLO22 Original

α = const. ____ FLO22 Width Body Influence

Fig. 4

4. Results

The TSD code alone and the TSD-FLO22 combination were both used for the flow computation around a number of configurations. The TSD code was used for the computation of the flow around a series of shapes of a fuselage of a supercritical aircraft, in order to choose a shape that produces less shock and thus less noise. Comparison with wind tunnel experiments shows good agreement. (e.g., Fig. 5).

The TSD code alone was used for computation of the flow around wing-body configurations, for wings with high sweep and low aspect ratio. Comparison with experiment is presented at Fig.6, for wing C, from the Lockheed wind tunnel models series (Ref.[7]). This wing has the sweep 45^o and the aspect ratio 2.8

The TSD code alone and the TSD-FLO22 coupling were extensively used for computation of the flow around a series of supercritical wing-body configurations, with a 20^{o} swept, high aspect ratio wing in a low position. A boundary layer was added to the wing shape, computed using simple sweep theory and knowledge of the approximate C_l value for all wing sections. Results are presented, for two wing sections (one inboard and one outboard) of one of the configurations, at Fig. 7.

REFERENCES

[1] Cole, J.D., "Twenty years of transonic flow ".Boeing Sci. Res., DI-82-0878, July 1969.

[2] Lomax, H., Bailey, F.R., and Ballhaus, W.F., "On the numerical simulation of three-dimensional transonic flow with application to the C-141" ,NASA TN D-6933 (1973).

[3] Hall, M.G. and Firmin M.C.P., "Recent developments in methods for calculating transonic flows over wings". ICAS PAPER No. 74 18 Haifa 1974.

[4] Boppe, C., "Calculation of transonic wing flows by grid embedding". AIAA 15th Aerospace Meeting. L.A., Calif., Jan 24-26, 1977.

[5] Boppe, C., "Computational transonic flow about realistic configurations". AIAA 16th Aerospace Sciences Meeting, 1978.

[6] A. Jameson and D. Caughey, "Numerical calculation of the transonic flow past a swept wing". Mathematics and Computing, NY Univ., 1977.

[7] B.L. Hinson and K.P. Burdges "Acquisition and application of transonic and far-field test data...". Report, Lockheed-Georgia Company. 1979.

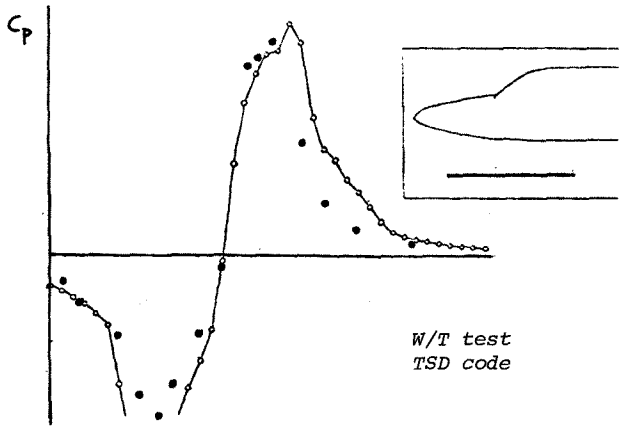

Fig. 5

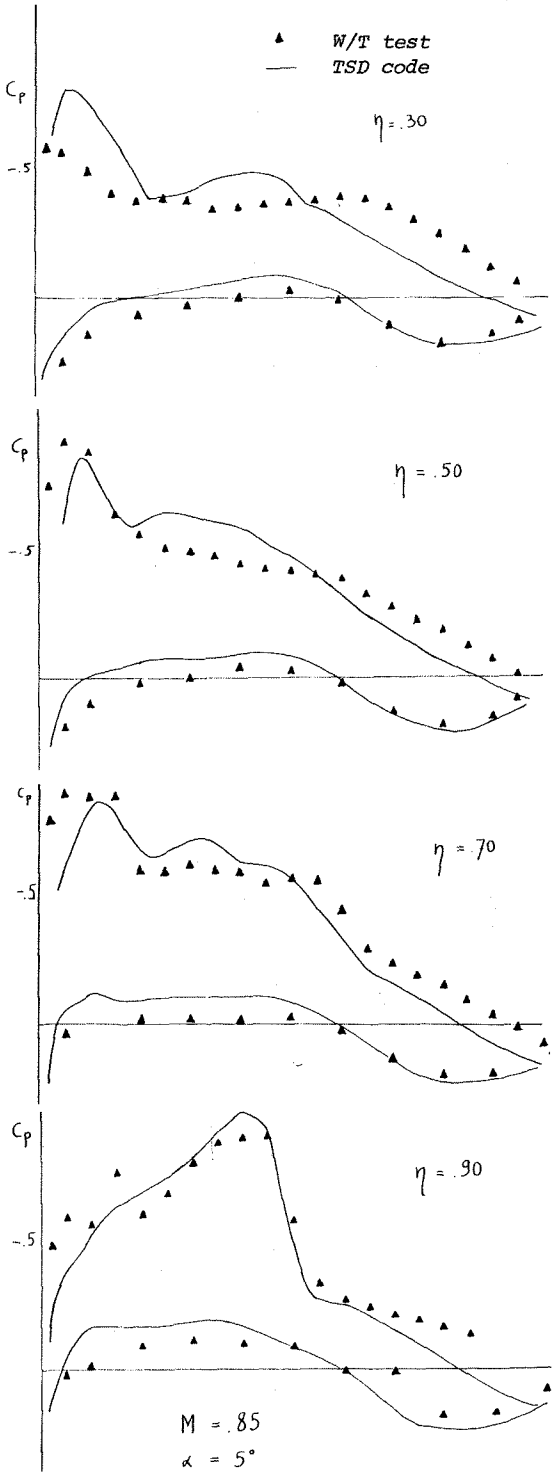

Fig. 6

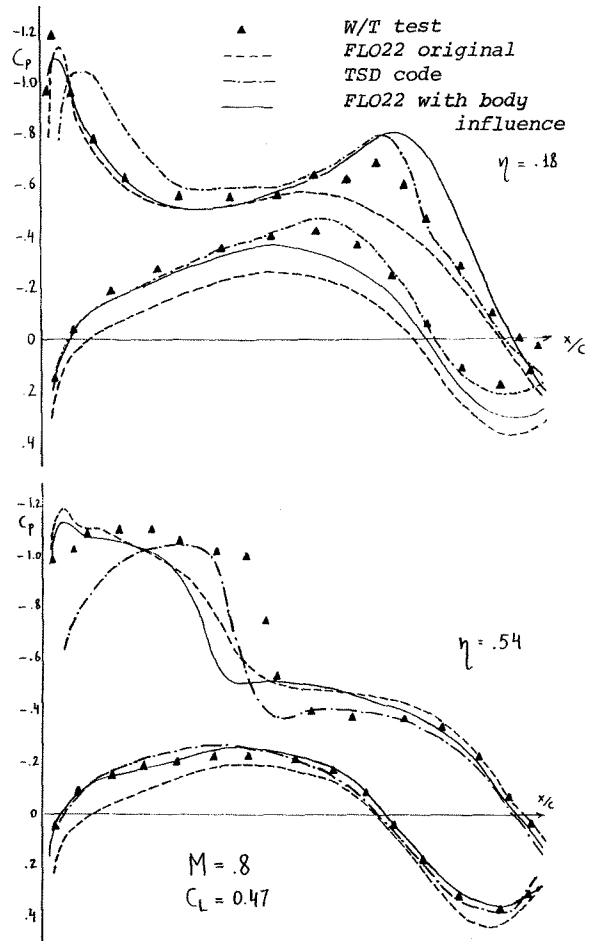

Fig. 7